Proc. NIPR Symp. Antarct. Meteorites, **2**, 252–267, 1989

VAPORIZATION OF SODIUM FROM A PARTIALLY MOLTEN CHONDRITIC MATERIAL

Taro SHIMAOKA and Noboru NAKAMURA

Department of Earth Sciences, Faculty of Science, Kobe University, 1-1, Rokkodai-cho, Nada-ku, Kobe 657

Abstract: In order to examine vaporization behavior of sodium for partially molten chondritic materials, heating experiments were carried out using two starting materials prepared from the Etter (L5) chondrite (grain-sizes: sample A, $\phi<10$ μm; sample B, $\phi=50$–90 μm) at temperatures of 1150–1450°C and pressure of 8×10^{-6} torr, and heating duration up to 160 min. Chemical analyses and petrographical examinations were carried out for starting materials and run products. The rates of vaporizations for sodium were estimated for partial melts (degree of melting=11–34%) at 1200–1400°C. Differences in the vaporization rates for the partially molten charges obtained from different starting materials were not detected clearly at the same temperatures. Systematically different trends of sodium vaporization rate are found between those obtained in this work and those previously reported for total melts (at 1450–1600°C) from similar starting materials (TSUCHIYAMA *et al.*, 1981). It appears that the vaporization mechanism of Na is basically the same in the temperature range from 1200 to 1600°C for partially to completely molten charges.

1. Introduction

Alkali metals are the moderately volatile lithophiles in high temperature processes, such as producing chondrules and/or their precursors and may be used as indicators of the physico-chemical conditions of high temperature gas/dust fractionation processes in the early solar system. In spite of high volatilities of alkali metals at chondrule melting temperatures, many chondrules from carbonaceous and unequilibrated ordinary chondrites have retained the volatile elements at the CI-chondritic level or higher (OSBORN *et al.*, 1974; GOODING, 1982, GROSSMAN and WASSON, 1982) and show the fractionated Na/K ratios relative to the CI-chondrite (GROSSMAN and WASSON, 1983) or an unfractionated Rb/K ratio in some cases (MISAWA and NAKAMURA, 1988a, b).

A number of vaporization experiments on silicate materials have been carried out to understand the elemental fractionations in meteoritic and lunar materials (DE MARIA *et al.*, 1971; GIBSON and HUBBARD, 1972; MASUDA and TANAKA, 1979; GOODING and MUENOW, 1977; IKRAMUDDIN *et al.*, 1977; NOTSU *et al.*, 1978; HASHIMOTO *et al.*, 1979; KREUTBERGER *et al.*, 1986). However, the vaporization experiments focused on alkali metals in chondrules have been quite limited. TSUCHIYAMA *et al.* (1981) performed a vaporization experiment of sodium on silicate materials with chondrule compositions in the temperature range of 1450–1600°C under the atmospheric pressure

with different oxygen fugacities. They have obtained the vaporization rate of sodium as a function of oxygen fugacity as well as temperature, and then discussed the melting and vaporization conditions for chondrule formation in the early solar nebula.

For further searches on behaviors of alkali metals during formation of chondrules in the nebula, we have undertaken vaporization experiments on alkali metals at lower temperatures (1150–1450°C) and a more reduced pressure than the previous work using the Etter (L5) chondrite. In this article, we report the results of chemical and petrographic examinations for the samples heated at 1150–1450°C, and present discussions on the vaporization rate of Na for partial to total silicate melts with chondrule composition.

2. Experimental

2.1. Apparatus

A new vaporization apparatus was constructed for the present purpose. Schematic illustration of the vaporization chamber is shown in Fig. 1. The furnace consists of a sample crucible ($\phi=7\times10$ mm) made of Ta-sheet (0.1 mm thick), a Ta-holder ($\phi=8\times60$ mm) supporting the crucible and a Ta-heater surrounded by Ta-thermal shields. The sample crucible is disposable for each heating run. The vacuum chamber was evacuated by a turbo molecular pump (Shimazu TMP-150) and a rotary pump (Shimazu MCD-160FA). The pressure monitored by an ionization gauge (ANELVA MIG-820) was normally pumping down to $1\text{–}5\times10^{-6}$ torr but adjustable using a metering valve connected to the chamber. Minor adjustment of the pressure (to 7.7×10^{-6} torr) in the heating chamber was, however, made with another metering valve which connected the heating chamber and the turbo pump in this work. Temperature of the crucible was monitored by a $W_{95}R_5$-$W_{75}Re_{25}$ thermocouple which had been calibrated against the melting temperature of pure gold metal (1064°C) *in vacuo*. The precision of temperature is estimated to be ±3°C.

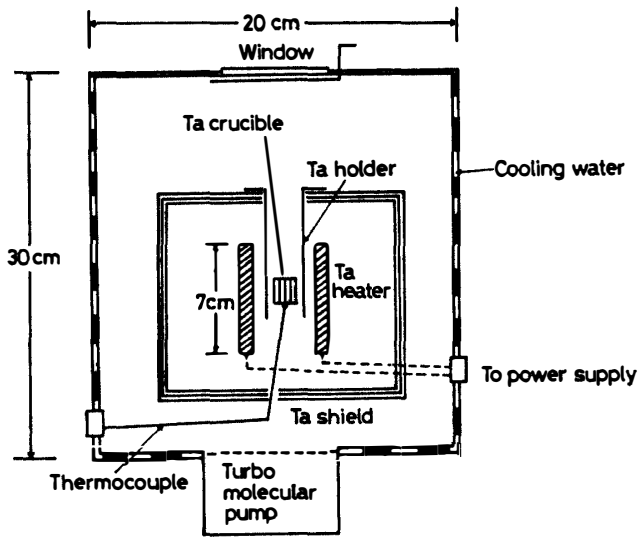

Fig. 1. Schematic illustration of the vaporization chamber.

2.2. Sample and heating procedures

Two kinds of starting materials with different grain-sizes were prepared from the Etter chondrite (L5); samples A (fine: $\phi<10$ μm) and B (coarse: $\phi=50$–90 μm). A 10 gram of the meteorite was first crushed to reasonable grain-sizes and then sieved using a teflon sieve of 50 μm. The sieved sample was further crushed to a fine powder ($\phi<10$ μm), and metal particles were removed with a magnet. This sample was used as one of starting materials (sample A) for heating experiments. The coarse-grained ($\phi>50$ μm) sample was sieved with a teflon sieve of 90 μm, and the sieved fraction (50 μm$<\phi<$90 μm) was used as the second starting material (sample B). Fine metal particles within silicate grains may have remained in the materials. Troilite was not intentionally separated but was partially removed during the sample processing. Each sample was carefully mixed up to form a homogeneous aliquot.

Much caution was exercised in the heating procedure as well as chemical analysis of trace amount of Na in run products to avoid the potential contamination of samples by alkali metals. The crucible was once baked in the furnace for 2–3 h at 1500°C before the run. About 50 mg of each sample was weighed and introduced in the furnace with a cleaned crucible. After pumping down the chamber to a pressure of 1–5×10^{-6} torr, the sample was degassed at a temperature below 900°C for about 2 h and then heated at a constant rate (29°C/min) up to a desired temperature (1150–1450°C) at the total pressure of 7.7×10^{-6} torr. After heating at the temperature for a certain duration (1–160 min), the power of the furnace was turned off and thus the sample was quenched with a cooling rate of 440–700°C/min.

Upon melting of the powdered samples at higher temperatures above 1300°C for fine-grained sample A or above 1400°C for coarse-grained sample B, the vesiculation occurs almost disruptively, and the sample crucibles were broken up. Despite several trials, heating experiments at such higher temperatures were not successful in this work. Although run product B heated at 1450°C was barely recovered but was not analyzed for Na because of the limited sample size.

2.3. Analysis

The run products were broken into fragments with an agate mortar. A few fragments were used for preparation of thin sections and the residual fragments (main part) were further crushed finely. A part of the powdered sample (15–40 mg) was weighed with a teflon bomb and then subjected to acid (HF-$HClO_4$) decomposition, dissolution in HCl and analysis of Na by atomic absorption spectroscopy (TERASHIMA, 1970) using an instrument Model Japan Jarrell-Ash AA-780.

The procedural blanks of Na obtained with and without a decomposition bomb are 0.72 and 0.63 μg, respectively, indicating that the major part of blank derived from impurities of reagents used for decomposition and dissolution of samples. Contributions of the blank to samples are less than 1% for analyses of starting materials, 10% for run products with relatively high Na contents (>500 ppm) but are 10–30% for samples with lower Na contents (<50 ppm). Therefore, analytical precisions of Na in run products with relatively low Na contents are highly dependent on uncertainties of amounts of blank correction. In addition, a possibility of fortuitous errors can not be excluded, which will be mentioned later.

Major chemical compositions of minerals and interstitial glass materials were determined with an electron microprobe analyzer (EPMA) (focused beam) (JEOL JCXA-733) at National Institute of Polar Research, and with scanning electron microscopes (SEM) equipped with an energy dispersive spectrometer (EDS) of Kyoto University (HITACHI-S530 with HORIBA-EMAX2200) and Okayama University (JEOL JSM-T220A with LINK QX-200J). They were operated at an accelerating voltage of 15–20 kV and a beam current of 1.5–12 nA. Petrographic examinations were also performed using SEM-EDS. The proportions of holes, glass materials and overgrowth rim materials to total samples were estimated from the SEM back-scattered electron images of run products using an on-line computer image reader. The total surface areas of holes were also estimated based on measurements of edges of holes by the same technique. Total volumes of heated samples (without holes) were estimated by dividing total sample weights by the assumed density of 3.3 (g/cm^{-3}).

3. Results

3.1. Starting material (the Etter chondrite)

Etter is an L5 chondrite containing microcrystalline aggregates of plagioclase (RUBIN *et al.*, 1983). The normative mineral abundances (excluding metal) calculated from the bulk chemical composition (RUBIN *et al.*, 1983) are; olivine (Fa_{35})=52.1%, hypersthene (Fs_{33})=24.8%, diopside ($En_{33}Fs_{16}Wo_{52}$)=4.8%, plagioclase (An_{25})=10.4% and troilite=6.2%. We have examined systematically alkali-rich phases by SEM-EDS and identified plagioclase (An_{13}), alkali-feldspar ($Ab_{69}Or_{31}$) and occasionally Fe-rich glassy materials (possibly aggregates of microcrystalline plagioclase and metal particles). Results of SEM-EDS analyses for Na-carrying phases together with the bulk composition of meteorite (metal-subtracted) are presented in Table 1. In order to test heterogeneities of major and minor elements, three to four splits taken from each strating material were analyzed for Na, Ca, Mg, and Fe (see Table 1). Analyses were carried out using mostly 20–30 mg size with one exception of analysis for 3.5 mg-size sample.

Standard deviations of Na concentrations in bulk samples are 3% for sample A and 1.5% for sample B. Differences of 6–8% in Na concentrations exist among small (3 mg) and larger (30 mg) samples but differences more than 10% were not detected among them (see Table 1). However, all the Na concentrations obtained for the coarse-grained sample B are systematically lower by 10% from those in sample A. Results of major element analyses by atomic absorption (Table 1) indicate that Ca, Mg, and Fe are distributed homogeneously in both starting materials, and that sample A is higher in Ca by 9% and lower in Mg by 8% than sample B. Therefore, results of analyses for major elements, specifically Ca, and minor element Na suggest that Na-carrying phases are distributed homogeneously in both starting materials at least for samples of more than 30-mg size, and that a minor fraction of alkali-rich phases was lost from sample B during the sample preparation (possibly in the mesh-sorting process).

The mean Na concentration (0.675%) in the fine-grained starting material A is in agreement with that (Na=0.68% in silicate fraction) reported by RUBIN *et al.* (1983)

Table 1. Chemical compositions of starting materials and the Etter (L5) chondrite (Values are expressed in wt%).

	Starting material*1 A (fine) $\phi<10\ \mu m$	Starting material*1 B (coarse) $\phi=50$–$90\ \mu m$		Etter (L5) Plagioclase	Etter (L5) Glassy material*2	Etter (L5) Alkali feldspar	Etter (L5) Bulk*3
Na	0.676	0.588	SiO_2	66.2	58.7	68.4	42.2
	0.655	0.576	TiO_2	0.0	0.0	0.0	0.1
	0.705	0.594	Al_2O_3	21.0	19.4	21.0	2.4
	0.665		Cr_2O_3	0.0	0.0	0.1	0.6
(mean)	0.675 ±0.021	0.586 ±0.009	CaO	2.4	3.5	0.2	2.0
			FeO	0.3	8.5	0.4	17.6
			MgO	0.1	0.6	0.0	26.6
Ca	1.36	1.23	MnO	0.0	0.0	0.0	0.3
	1.37	1.27	K_2O	0.2	0.3	3.9	0.1
	1.35		Na_2O	9.7	7.4	5.8	0.9
			FeS				6.1
Mg	15.2	16.4	H_2O+C				1.1
	15.3	15.2					
	15.2		Total	99.9	98.4	99.8	100.0
Fe	15.5	11.9					
	15.2	13.2					

*1 Prepared from the metal-removed Etter chondrite.

*2 Considered to be microcrystalline aggregates of plagioclase and metal particles but the chemical compositions are expressed as oxide form.

*3 Metal-subtracted composition (adjusted to 100%) reported for the Etter (L5) chondrite (RUBIN *et al.*, 1983).

for the bulk Etter chondrite. The chemical compositions of the bulk samples and minerals and SEM observation indicate that the majority of feldspar minerals are plagioclase. Assuming that Na exists solely as plagioclase (An_{25}) in the starting materials, the plagioclase contents are calculated to be 11.1% and 9.6% for starting materials A and B, respectively.

The troilite contents in starting materials were not accurately determined in this work but were roughly estimated to be 3% and 0.8% for samples A and B, respectively, from the back-scattered electron images. This observation is also consistent with higher Fe content (15% in sample A obtained by atomic absorption. Most of troilite was found to exist as discrete grains and discrete metal grains are rare in sample A, while some metal grains together with troilite exist within silicate grains in a few cases in sample B.

From the above observations we suggest that chemical and mineral compositions of two starting materials with different grain-sizes are sufficiently homogeneous, and minor but significant differences, particularly in plagioclase and troilite contents, exist between them.

3.2. Melting textures of heated samples

Some examples of SEM back-scattered electron images of run products are shown in Fig. 2. They are composed mainly of olivine (light dark), pyroxene (dark), glass (irregularly shaped light portion), troilite or metal (rounded light portion) and holes

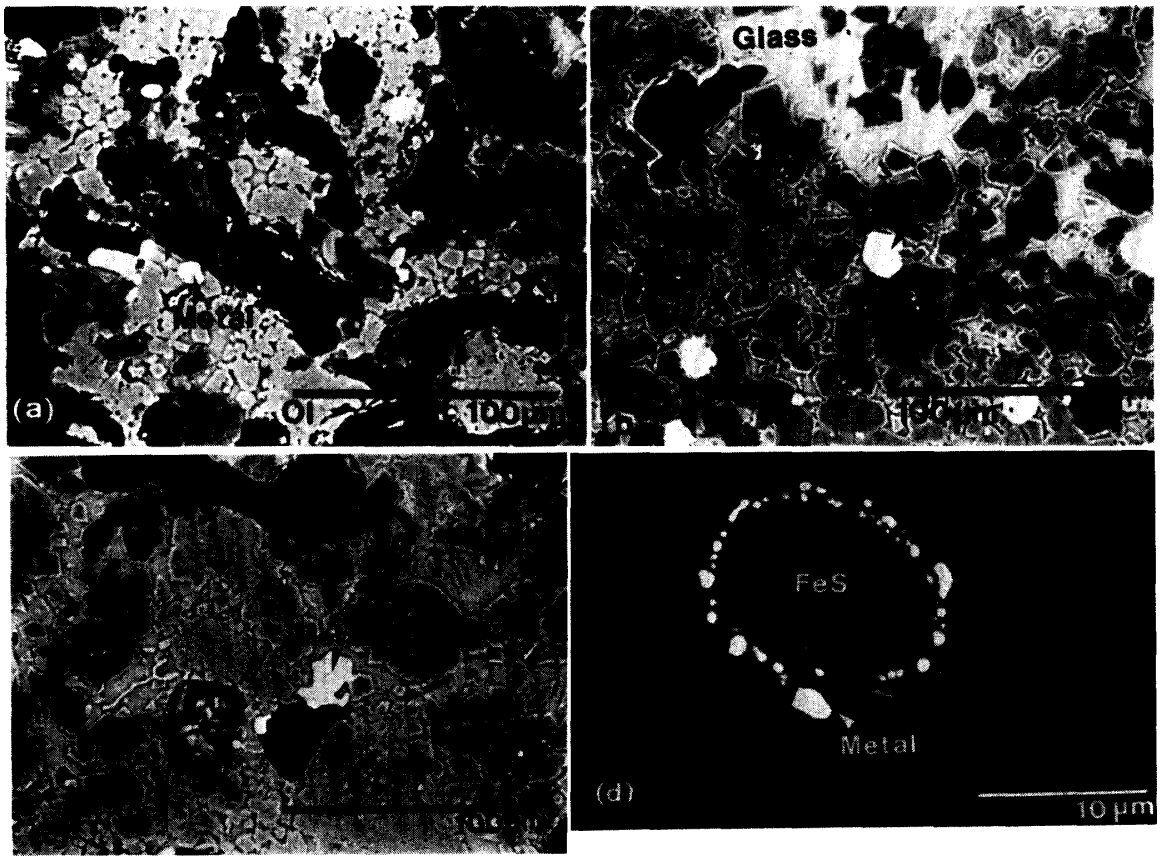

Fig. 2. SEM back-scattered electron images of the heated samples. (a) Run product obtained from the fine-grained starting material A at 1200°C for 160 min. Many holes (black), glass materials representing partial melt (light), olivine (light dark) and pyroxene (dark) grains with overgrowth rims are noted. (b) Run product from sample A at 1300°C for 160 min. Rounded troilite grains (white) embedded in melt and mineral grains are often encountered. (c) Run product obtained from the coarse-grained starting material B at 1300°C for 40 min. Metal grains formed by decomposition of troilite are occasionally recognized. (d) Rounded troilite grain (dark area) surrounded by metal gains (almost no Ni) which embedded in glassy material are often encountered in run products of 1300°C from sample A. The texture suggests that troilite grains were trapped by partial melts and thus decomposition of sulfide was suppressed.

(black). The following three textural features are worth noting here.

(1) All run products contain abundant holes (10–60% in area). The areal proportions of holes to the total sample measured from back-scattered electron images are presented in Table 2. It is pointed out that run products of the coarse-grained starting material B have more abundant holes compared with those of the fine-grained starting material A at same temperatures, and that, in general, heated samples obtained at higher temperatures have less abundant holes. Therefore, it is likely that most holes were not formed by vesiculation of heated samples but represent open spaces unfilled with partial melts, which will be discussed later.

For later discussion, the total surface areas of holes were assumed to be the square of edge length of holes estimated from SEM back-scattered electron images. Proportions of surface areas of melts to total areas of holes were not able to estimate with

Table 2. Bulk Na concentrations and percent fractions of glasses and holes in run products.

Run No.	Temp. (°C)	Duration (min)	Weight loss*1 (%)	Holes*2 (%)	Total surface area (cm^2)	Deg. of*4 p. melt (%)	Na (ppm)
37 A	1200	70	3.0	31.1	6.16 (0.25)*3	11.7	450
35 A	1200	160	3.3	33.2	5.50 (0.27)	13.0	129
29 A	1300	40	2.8	6.5	2.40 (0.30)	25.2	1170
30 A	1300	56	3.0	11.8	2.59 (0.26)	22.1	87
28 A	1300	80	3.3	10.2	2.78 (0.29)	31.1	98
27 A	1300	120	3.3	11.0	4.28 (0.34)	22.3	462
32 A	1300	138	3.8	9.7	2.49 (0.26)	24.2	6
31 A	1300	160	3.6	8.8	2.57 (0.27)	32.3	109
52 B	1150	60	1.8	41.0	4.09 (0.20)	11.8	
51 B	1200	30	1.9	41.6	3.24 (0.20)	18.5	2360
53 B	1250	30	1.8	58.5	3.59 (0.19)	10.9	354
42 B	1300	20	2.0	56.5	5.25 (0.21)	32.3	1120
38 B	1300	40	2.0	27.3	2.26 (0.21)	17.2	
39 B	1400	10	2.8				
40 B	1400	5	2.3		1.51 (0.21)		
41 B	1400	2	1.9	13.5	1.41 (0.20)	33.6	65
44 B	1410	2	2.5		1.25 (0.21)		
43 B	1450	1			0.31 (0.19)		

*1 $100\times\{1-$(wt. of run product)/(wt. of starting material)$\}$.

*2 Areal proportion of holes to the total charge determined by an on-line computer image reader from the back-scattered electron images.

*3 Surface areas of outside of charges calculated from weight of charges.

*4 Estimated from combined proportion of glass and overgrowth rim material total charge.

any confidence in this work and thus used as an parameter (see equation (4)). The surface area outside of heated sample was estimated to be that of one half of surface area of assumed sphere with density of 3.3 (g/cm^3).

(2) The presence of significant amounts of interstitial glass in heated samples and the estimated solidus temperature of 1100°C for an L-chondritic material including troilite (TAKAHASHI, 1983) suggest that partial melting was occurring during the heating. As inferred from the presence of overgrowth rim material ssurrounding mineral grains adjacent to glass (light-colored portions in Fig. 2), the cooling rate (600°C/min) in this work has not been fast enough to quench all the partial melts. The Fa contents of overgrowth olivine grains are 31–35% for heated samples at 1200–1400°C and are systematically higher than those of adjacent olivines (Fa=18–29%). The possible local heterogeneities of chemical compositions of glass materials were also examined by SEM-EDS but were not detected clearly, suggesting that melts had been sufficiently homogenized except for very narrow areas.

The width of rim materials measured on back-scattered images are 0.9 ± 0.3 μm for 1150°C, 1.0 ± 0.3 μm for 1200°C 1.1 ± 0.3 μm for 1250°C, 1.2 ± 0.3 μm for 1300°C and 1.4 ± 0.3 μm for 1400°C. The areal proportions of overgrowth rim materials estimated from back-scattered images correspond to 20–50% of total amounts of glass and rim materials. The degrees of partial melting were estimated from the

combined proportions of glass and rim materials to the total charge. The degrees of melting are 11% for 1150°C, 12–19% for 1200°C, 20–32% for 1300°C and 34% for 1400°C (see Table 2). Because of heterogeneous distributions of holes and rim materials, estimated proportions of holes and degrees of partial melting mentioned above may contain considerably large uncertainties (20–30%).

(3) The troilite grains were scarce in run products from the coarse-grained starting material B at all temperatures and also rare in run products from the fine-grained starting material A at 1150 and 1200°C, but instead metal grains poor in nickel were occasionally encountered (Figs. 2a and 2c). Except for these run products, run products at 1300°C from sample A contain much more abundant troilite grains and less abundant metal grains (Fig. 2b). The metal grains in samples (A) at 1300°C are poor in nickel and accompanied by troilite. Some of the troilite grains were surrounded by small metal grains (Fig. 2d), showing decomposition of troilite to form the metal.

The presence of more abundant troilite in sample A heated at the higher temperature (1300°C) than 1200°C and 1150°C appeared misleading but was confirmed for several run products. We suggest that the perplexing phenomenon recognized here is not accidental nor due to heterogeneity of starting materials and/or run products. TAKAHASHI (1983) reported similar textural features for partial melts of L-chondrite formed at temperatures above clinopyroxene liquidus at high pressure, and suggests that due to a large surface energy relative to that of a silicate melt the metal/sulfide melts become globes of various sizes. Therefore, it is considered that in the experiment of sample A at 1300°C the melting and the filling of open spaces with partial melts may have resulted in trapping of troilite melts within the silicate melts and then decomposition of troilite was suppressed but a part of troilite dissolved in melts. This would explain why only the run products from sample A heated at the higher temperature have retained more abundant troilite but less metal grains and have glass materials with significantly high contents (0.2–0.3 wt%) of sulfur.

These textural observations also lead us to an interesting suggestion for origin of metal and troilite in many chondrules (GROSSMAN and WASSON, 1985) that some metal grains were formed from troilite which had been trapped in partial melts formed by instantaneous heating (flash-heating?) of dust balls.

From the above observation, it was found that partial melting of silicate grains and decomposition of troilite occurred during the heating at 1150–1400°C. Because of a low degree of melting (<20%) at temperatures below 1300°C the interstitial spaces were not filled perfectly with the melt, or interstitial spaces in coarse-grained sample B were too much to be filled perfectly with partial melts even if heated at higher temperatures. Then, more abundant holes remained unfilled in coarse-grained sample B compared with fine-grained sample A. Decomposition of troilite eutectic melt was effectively processed through holes and then some metal grains were formed. On the other hand, at higher temperature (1300°C), the fine-grained starting material A may have had less interstitial open space so that the open spaces were more easily filled with melts.

3.3. *Chemical composition of partial melts*

The Fo contents (%) in olivine grains range from 72 for 1200°C to 80±2 for 1400°C and are homogeneous at given temperatures. Most pyroxene grains are low-Ca orthopyroxene with compositions of Fs_{21-27}. Interstitial glass materials are normally poor in sulfur (almost below the detection limit of SEM-EDS) but run products from samples A heated at 1300°C have systematically higher sulfur contents (0.2–0.3 wt%). Solubility of sulfur in a basaltic melt at a given pressure and f_{O_2} is a function of the FeO content in the melt (WENDLANDT, 1982). About 0.2 wt% of sulfur is expected in partial melts formed after extensive melting of L-chondrite at high pressures (TAKAHASHI, 1983). The similarly high sulfur contents observed in the partial melt at 1300°C indicate that sulfur dissolved in the partial melts by decomposition of sulfide melts.

Chemical compositions of partial melts were estimated based on EPMA analyses of glass and rim materials. The composition range of partial melts is 45–50 wt% SiO_2, 9–5 wt% contain Al_2O_3, 7–5 wt% CaO, 15–25 wt% FeO and 15–17 wt% MgO. Thus, chemical compositions of partial melts are systematically fractionated with heating temperature. The chemical compositions and degree of melting suggest that at temperatures above 1200°C plagioclase was completely exhausted and significant amounts of olivine and pyroxene melted.

3.4. *Concentration of Na in the heated samples*

The results of analyses for Na in the bulk run products are presented in Table 2 and Fig. 3. All concentrations are corrected for analytical blanks. The run products from samples A heated at 1200 and 1300°C were examined systematically with varying heating duration. Except for two samples (27A and 31A), the Na concentrations in run products decrease with an increase of heating duration. Because of a large blank contribution (~70%), concentration of Na in 32A (5 ppm) contains large uncertainties and is thus the lower limit of atomic absorption analyses in this work. The expected total amount of Na in 31A (sample weight used for analysis=11 mg) from the general trend of samples heated at 1300°C is calculated to be 0.0008 μg which is far below the limit of our analytical capability. The blank value of 0.72 μg corresponds to 65 ppm for 31A and thus the observed value of 100 ppm is even higher than expected from contamination. In view of potential variations of blank during analytical processes, the observed high value is not acceptable as a true one.

The Na concentration (460 ppm) in 27A is about several orders of magnitude larger than the expected value (7 ppm). This too high Na concentration is not explained solely as due to blank effect, even if variability of blank is considered. At present, we have no obvious interpretation for the reason, but heterogeneities of starting materials and/or run products may be worth considering as one of possibilities. However, such large Na heterogeneity in starting materials can be hardly accepted because variations of Na concentrations in starting materials (A and B) are quite limited (up to 20%) (see Table 1). On the other hand, because of limited size and too low Na concentration, duplicate analyses of the run product were not carried out. In addition, we have not repeated heating experiments to confirm the above observation. Hence, we can not rule out a possibility that the observed high Na content in

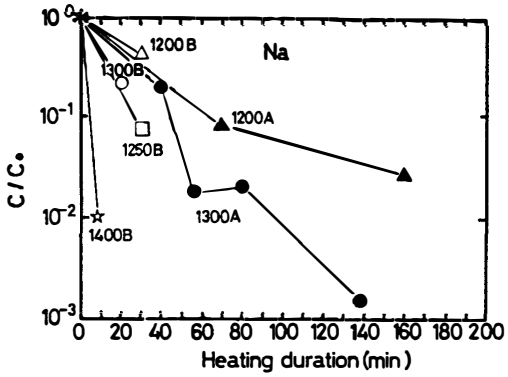

Fig. 3. Plot of relative concentration of Na in the heated samples to starting materials as a function of heating duration.

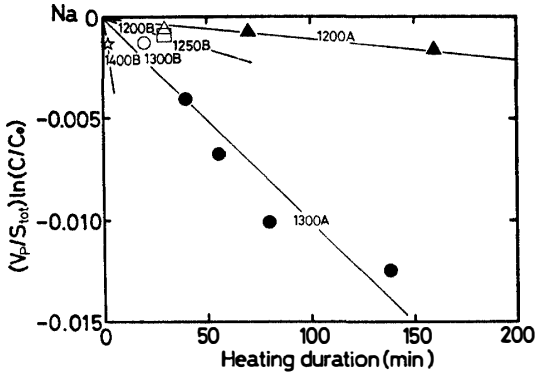

Fig. 4. Plot of relative concentration of Na in heated samples corrected for effects of holes and partial melts as a function of heating duration.

27A was caused by an extreme heterogeneity in the run product.

In conclusion, the Na data obtained for these two samples (27A and 31A) are not considered to represent concentrations in samples heated at 1300°C for longer duration. Therefore, these Na data are omitted from Fig. 3 and in the later discussion. In Fig. 3, the too much depletion of Na data point of 1250°C compared with data points of 1300°C appears unusual but is found to be reasonable if surface areas and degrees of partial melting of charges are corrected (see Fig. 4).

4. Discussion

4.1. Vaporization rate of Na for the partially molten charge

TSUCHIYAMA *et al.* (1981) reported that at temperatures above 1450°C the Na vaporization from silicate melts with chondrule composition is controlled by the loss of the element from the surface of charge, that is, the diffusion of the element from the interior of charge to the surface is fast enough. For the partially molten charges in question, we assume that the rate of Na vaporization is proportional to the surface area of the partial melt useful for vaporization, S, and to the concentration of Na in the partial melts, C_p. Then the following equation is obtained;

$$dM_p/dt = -kSC_p = -kS(M_p/V_p) \tag{1}$$

where M_p and V_p are the amount of Na in the partial melt and the volume of the partial melt. k is the vaporization rate of Na which is a function of temperature,

total pressure, oxygen partial pressure and chemical composition. Assuming that during heating at a given temperature Na is all contained in the partial melts, and the surface area and the volume of the partial melt and the charge, are unchanged, then eq. (1) is solved as follows:

$$\int_{M_0}^{M} \mathrm{d}M/M = -\int_0^t kS/V_\mathrm{p}\mathrm{d}t \tag{2}$$

and then

$$\int_{M_0}^{M} \mathrm{d}M/M = \ln(M/M_0) = \ln(C/C_0)$$

$$\ln(C/C_0) = -k(S/V_\mathrm{p})t \tag{3}$$

where $M(M_0)$ and $C(C_0)$ are amount and concentration of Na for bulk charge at duration t (or at $t=0$), respectively. Therefore, the vaporization rate for the partially molten charge is found to be expressed as the similar form as the case of the totally melted charge (TSUCHIYAMA *et al.*, 1981). However, the meaning of the calculated rates using the above equation is solely dependent on the validity of the above-mentioned assumptions. For application of eq. (3) to the present experiments the following three assumptions must be appropriate; during the vaporization of sodium (1) all sodium contained in bulk sample is located in the partial melts, (2) surface area of partial melt is constant and (3) volume of partial melt is constant.

4.2. Application of vaporization equation

The equilibrium solid/liquid partition coefficients of Na for natural rock-forming minerals are less than 0.01 for olivine, 0.08 for orthopyroxene, 0.27 for clinopyroxene and 1.2 for plagioclase (MATSUI *et al.*, 1977). As mentioned earlier, all run products in this work consist mainly of glass and olivine with less abundant (<20%) orthopyroxene. Plagioclase is completely exhausted to melt phase. Using the mineral compositions of run products and the partition coefficient of Na, the upper limit of total sodium contents in mineral phases is calculated to be 5% of all sodium in charges. On the other hand, in view of the homogeneous distribution of Fa in olivines and Fs in pyroxene grains in run products of different heating durations in most cases, partial melting is considered to have occurred nearly in an equilibrium condition. Thus, the assumption (1) is considered to be valid, although this was examined for run products from samples B at 1150, 1250, and 1400°C.

The vaporization of Na is considered to have been processed mostly from surfaces of holes and partly from outside of charges, if all the surface areas measured are useful for vaporization. The total surface areas (S_tot) of charges estimated from back-scattered electron images are given in Table 2. The surface area useful for vaporization (hereafter called effective surface area), however, is limited to surface areas of partial melts on the outside and in the holes which are connected to the outside. The overall proportion (f) of effective surface areas of partial melts (S) to total surface areas (S_tot) and their time dependencies are unknown. As found in Table 2, proportions of holes, total surface areas and degrees of partial melting are roughly constant at given temperatures. We, tentatively, accept the second assumption (2)

and use the effective surface area for S in eq. (3).

Hence, $S=f\cdot S_{tot}$=const. (f=const.) and thus

$$\ln (C/C_0)=-k(f\cdot S_{tot}/V_p)t \quad (4)$$

From back-scattered electron images of heated samples, the f values are estimated to be significantly smaller than unity but were not estimated in this work.

The weight loss during vaporization is 1.8–3.8% of total charge (see Table 2). Since volatile components of 1.1% (see Table 1) are considered to have been lost before partial melting, the net weight loss during melting is estimated to be 0.7–2.7% by subtracting this value. Assuming that this weight loss was due to vaporization of partial melts, volume changes of partial melts during vaporization are calculated to be 7% or smaller (the density of partial melt is assumed to be 2.5 g/cm^3). Therefore, considering large uncertainly of other parameters such as effective surface areas, the third assumption seems to be relatively reasonable.

In order to test validity of this data assessment, the volume and surface area corrected ln $[C/C_0]$ values were plotted against the heating duration in Fig. 4. Although uncorrected data points (typically data point of 1250°C) in Fig. 3 show unusual variations, the distribution of data points after correction for melt volumes and total surface areas is now appropriate and shows more clear linear trends in Fig. 4, as expected from eq. (4). Systematic differences in data distributions between starting materials of different grain sizes are not clearly recognized here.

In spite of relatively large uncertainties of surface areas and melt volumes, the expected linear trends are obtained at 1200 and 1300°C in Fig. 4, suggesting that our data analysis is basically correct, and hence, the initial assumption that the rate-determining process is the vaporization from the partial melt may also be substantiated.

4.3. Vaporization rates of Na

The rates of Na vaporization as a function of f value are calculated using combined data sets for run products of samples A and B at 1200 and 1300°C. For calculation, it is assumed that a regression line passes through the origin. Unfortunately, each heating experiment at 1250 and 1400°C was performed only for one heating duration and thus the vaporization rate calculated from each one data point is of only tentative significance. The calculated values are given in Table 3, and an Arrhenius plot of vaporization rate is shown in Fig. 5, together with those obtained by TSUCHIYAMA *et al.* (1981).

Table 3. Calculated vaporization rate (cm^3/min cm^2) of Na as a function of f.*

f	1200°C	1250°C	1300°C	1400°C
1	1.0×10^{-5}	3.0×10^{-5}	1.0×10^{-4}	6.6×10^{-4}
0.2	5.2×10^{-5}	1.5×10^{-4}	5.0×10^{-4}	3.3×10^{-3}
0.1	1.1×10^{-4}	3.0×10^{-4}	1.0×10^{-3}	6.6×10^{-3}
0.05	2.1×10^{-4}	6.0×10^{-4}	2.0×10^{-3}	1.3×10^{-2}

* f represents assumed proportion of the effective surface area of partial melt (S) to total surface area of the run product (S_{tot}) (see text). Vaporization rates were calculated using equation (4).

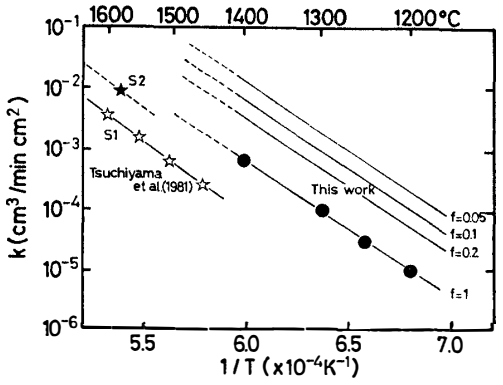

Fig. 5. Arrhenius plot of the rates of Na vaporization obtained in this work and by TSUCHIYAMA et al. (1981). Symbols of solid circles were obtained for partially molten charges in this work assuming $f=1$ (f=assumed proportion of the effective surface areas of partial melts to total surface areas). The parallel lines with these data represent assumed vaporization rates at different f values.→Symbols of solid and open stars represent data from TSUCHIYAMA et al. (1981) for samples 1 and 2, respectively, in the temperature range of 1450–1600°C at the oxygen partial pressure of $10^{-9.2}$ atm.

Four data points at given f values show a linear trend as generally expected in this type of thermal data for a narrow temperature range. Extraporating the regression line, the rate of Na vaporization is calculated to be $1.8\times10^{-3}/f$ (cm³/min·cm²) ($f<1$) at 1456°C. This value is significantly larger than that (2.6×10^{-4}) obtained by TSUCHIYAMA *et al.* (1981) for sample 1 (1456°C, $\log[f_{O_2}]=-9.2$). On the other hand, the extrapolated value of $1.4\times10^{-2}/f$ at 1586°C is even higher than that (8.8×10^{-3}) obtained by the same authors for sample 2 at the same temperature ($\log[f_{O_2}]=-9.2$). Depending on the f value, the calculated rates for the present experiments substantially shift to much higher.

The reason of the higher values of vaporization rate observed in this work compared to those by TSUCHIYAMA *et al.* (1981) may be due to differences in 1) total pressure and/or the oxygen fugacity, 2) the chemical composition of charge and 3) the vaporization mechanism of Na between two experimental systems. In order to elucidate these factors, more extensive works may be needed. However, some indications could be obtained from the following discussion.

TSUCHIYAMA *et al.* (1981) obtained the vaporization rates at the atmospheric pressure which is much higher than the total pressure (7.7×10^{-6} torr) at which the present experiments were carried out. The effect of the total pressure on the vaporization rate of sodium has not been known but is considered to be significant. In general, the vaporization rates are considered to be enlarged at more reduced pressures. Therefore, it is possible that the higher vaporization rates obtained in this work compared with those by TSUCHIYAMA *et al.* (1981) are partly due to the much lower total pressure in this work.

The effect of the oxygen partial pressure on the vaporization rate has been experimentally clarified (TSUCHIYAMA *et al.*, 1981). The oxygen partial pressure within the heating chamber in this work is considered to be controlled by 1) residual air, 2) released gas from partial melts, 3) Fe-FeO buffer of charges and 4) Ta-Ta_2O_5 buffer of Ta-crucible, Ta-heater and Ta-tube.

The total pressure of 7.7×10^{-6} torr corresponds to 2×10^{-9} atm, if all the residual gas in the chamber is assumed to be air. Decomposition of silicate and sulfide melts may yield oxygen and sulfur, respectively. The estimated proportions of silicate and sulfide melts from weight loss (Table 1) are variable from sample to sample for different starting materials and heated at different temperatures. If the released

gasses from partial melts are the main components which controlled the vaporization rates, the smooth variation of the observed vaporization rates in Fig. 4 is rather difficult to understand, which is in turn suggesting that the factor 2) is not too much important. On the other hand, the gas in the chamber directly contacted with partial melts, olivine, pyroxene and minor Fe metal/sulfide. Then, the reaction of Fe with mafic minerals may work as an oxygen buffer. The estimated oxygen partial pressures are 10^{-13} at 1200°C and 10^{-11} atm at 1400°C (JOHNSON, 1986). Furthermore, if the Ta-materials work as the Ta-Ta_2O_5 buffer, then the oxygen partial pressures are calculated to be 10^{-20} at 1200°C and 10^{-17} atm at 1400°C.

In view of systematically high vaporization rates observed in this work, the reaction which controlled the oxygen partial pressure may have prevailed quite consistently through all the heating experiments. Thus, a role of sulfur produced by decomposition of troilite may not be important. The most important reactions may be that of the partially molten charges themselves and/or Ta-Ta_2O_5 buffer. If this is the case, the oxygen partial pressures in this experiments are estimated to be a few to several orders of magnitude smaller than that in TSUCHIYAMA *et al.* (1981), which is relatively consistent with the higher vaporization rates of Na obtained in this work.

The chemical compositions of partial melts obtained in this work are significantly different from bulk compositions of total melts examined by TSUCHIYAMA *et al.* (1981). Particularly, the differences in Al and Ca are worth noting. These authors recognized significantly large differences in vaporization rates for starting materials with different chemical compositions but they did not clarify the cause. In this work, we also noted systematically fractionated chemical compositions of partial melts produced at different temperatures, but did not detect chemical effects on vaporization rates clearly. Therefore, we can not rule out a possibility that the systematically higher vaporization rates obtained in this experiment were partly due to fractionated chemical compositions of partial melts.

Because of incomplete experimental data obtained in this work, vaporization rates of sodium estimated here include relatively large uncertainties and may need further evaluation. The present data analysis, however, suggested that the vaporization rates of sodium obtained in this work in the lower temperature range (1200–1400°C) seem to be consistent with those by TSUCHIYAMA *et al.* (1981) at higher temperatures (1450–1600°C), which is in turn suggesting that the vaporization mechanism of Na is basically the same for the partially to totally molten charges of chondritic materials in the temperature range from 1150 to 1600°C. In order to clarify more details of vaporization mechanism mentioned here, further experiments are required.

Acknowledgments

We are indebted to Drs. A. TSUCHIYAMA, M. KITAMURA and Prof. N. MORIMOTO, Kyoto University, to Profs. Y. MATSUI and H. HONMA, Okayama University, and to Dr. H. KOJIMA, National Institute of Polar Research, for allowing us to use the SEM-EDS or EPMA. The advice and assistance regarding SEM-EDS analyses and data synthesis given by Dr. TSUCHIYAMA are particularly acknowledged. One of the

authors (T.S.) thanks Prof. N. FUJII and Dr. T. NAKANO, Kobe University, for the encouragement during the course of the work as well as the permission of the access to the on-line computer image reader. We thank anonymous reviewers for their constructive comments on the manuscript.

This work was supported in part by the Grant-in-Aid for Scientific Research on Priority Areas (Origin of the Solar System) of the Ministry of Education, Science and Culture, Japan (No. 6311003).

References

DE MARIA, G., BALDUCCI, G. and PIACENTE, V. (1971): Mass spectrometric investigation of the vaporization process of Apollo 12 lunar samples. Proc. Lunar Planet. Sci. Conf., 2nd, 1367–1380.

GIBSON, E. K., Jr. and HUBBARD, N. J. (1972): Thermal volatilization studies on lunar samples. Proc. Lunar Planet. Sci. Conf., 3rd. 2003–2014.

GOODING, J. L. (1982): Survey of chondrule average properties in H-, L-, and LL-group chondrites; Are chondrules the same in all unequilibrated ordinary chondrites? Chondrules and Their Origins, ed. by E. A. KING. Houston, Lunar Planet. Inst., 61–87.

GOODING, J. L. and MUENOW, D. W. (1977): Experimental vaporization of the Holbrook chondrite. Meteoritics, **12**, 401–408.

GROSSMAN, J. N. and WASSON, J. T. (1982): Evidence for primitive nebular components in chondrules from the Chainpur chondrite. Geochim. Cosmochim. Acta, **46**, 1081–1099.

GROSSMAN, J. N. and WASSON, J. T. (1983): Refractory precursor components of Semarkona chondrules and the fractionation of refractory elements among chondrites. Geochim. Cosmochim. Acta, **47**, 759–771.

GROSSMAN, J. N. and WASSON, J. T. (1985): The origin and history of the metal and sulfide components of chondrules. Geochim. Cosmochim. Acta, **49**, 925–939.

HASHIMOTO, A., KUMAZAWA, M. and ONUMA, N. (1979): Evaporative metamorphism of primitive dust material in early solar nebula. Earth Planet. Sci. Lett., **43**, 13–21.

IKRAMUDDIN, M., MATZA, S. and LIPSCHUTZ, M. E. (1977): Thermal metamorphism of primitive meteorites V. Ten trace elements in Tieschitz H3 chondrite heated at 400–1000°C. Geochim. Cosmochim. Acta, **41**, 1247–1256.

JOHNSON, M. (1986): The solar nebula redox state as recorded by the most reduced chondrules of five primitive chondrites. Geochim. Cosmochim. Acta, **50**, 1497–1502.

KING, E. A. (1982): Refractory residues, condensates and chondrules from solar furnace experiments. Proc. Lunar Planet. Sci. Conf., 13th (J. Geophys. Res., Suppl. **55**, A429–434).

KREUTZBERGER, M. E., DRAKE, M. J. and JONES, J. H. (1986): Origin of the Earth's Moon; Constraints from alkali volatile trace elements. Geochim. Cosmochim. Acta, **50**, 91–98.

MASUDA, A. and TANAKA, T. (1979): Experimental studies on behaviors of major and minor lithophile elements in vaporization under evacuated condition. Meteoritics, **14**, 13–28.

MATSUI, Y., ONUMA, N., NAGASAWA, H., HIGUCHI, H. and BANNO, S. (1977): Crystal structure control in trace element partition between crystal and magma. Bull. Soc. Fr. Mineral. Cristallogr., **100**, 315–324.

MISAWA, K. and NAKAMURA, N. (1988a): Demonstration of REE fractionations among individual chondrules from the Allende (CV3) chondrite. Geochim. Cosmochim. Acta, **52**, 1699–1710.

MISAWA, K. and NAKAMURA, N. (1988b): Rare earth elements in chondrules from the Felix (CO3) chondrite; Comparison with Allende (CV) chondrules. Proc. NIPR Symp. Antarct. Meteorites, **1**, 215–223.

NOTSU, K., ONUMA, N., NISHIDA, N. and NAGASAWA, H. (1978): High temperature heating of the Allende meteorite. Geochim. Cosmochim. Acta, **42**, 903–907.

OSBORN, T. W., WARREN, R. G., SMITH, R. H., WAKITA, H., ZELLMER, D. L. and SCHMITT, R. A. (1974): Elemental composition of individual chondrules from carbonaceous chondrites,

including Allende. Geochim. Cosmochim. Acta, **38**, 1359–1378.

RUBIN, A. E., REHFELDT, A., PETERSON, E., KEIL, K. and JAROSEWICH, E. (1983): Fragmental breccias and the collisional evolution of ordinary chondrite parent bodies. Meteoritics, **18**, 179–196.

TAKAHASHI, E. (1983): Melting of a Yamato L3 chondrite (Y-74191) up to 30 kbar. Mem. Natl Inst. Polar Res., Spec. Issue, **30**, 168–180.

TERASHIMA, S. (1970): Determination of sodium, potassium, magnesium, calcium manganese and iron in the silicate rocks and terrestrial water by atomic absorption spectrophotometry. Bull. Geol. Surv. Jpn., **21**, 693–707.

TSUCHIYAMA, A., NAGAHARA, H. and KUSHIRO, I. (1981): Volatilization of sodium from silicate melt spheres and its application to the formation of chondrules. Geochim. Cosmochim. Acta, **45**, 1357–1367.

WENDLANDT, R. F. (1982): Sulfide saturation of basalt and andesite melts at high pressures and temperatures. Am. Mineral., **67**, 877–885.

(Received September 22, 1988; Revised manuscript received May 1, 1989)